Supporting Information

Multiplex MicroRNAs Imaging in Living Cell Using DNA-Capped-Au Assembled Hydrogels

Xiangdan Meng, Kai Zhang, Wenhao Dai, Yu Cao, Fan Yang, Haifeng Dong and Xueji Zhang**

Non-invasively imaging multiplex microRNAs (miRNAs) in living cells is pivotal to understand the physiological functions and pathological development due to key regulator roles of miRNA in gene expression. However, smart delivery system with large gene loading capacity, biocompatibility and responsiveness remains a significant challenge. Herein, we successfully incorporate DNA-capped Au nanoparticles (NPs) and their complementary fluorescent DNA sequences into a porous 3D hydrogel network (AuDH), in which hairpin-locked DNAzyme and active metal irons were loaded (AuDH/M^{n+}/H) for simultaneously imaging multiplex miRNA in living cells. After transfecting into cells, the specific miRNA trigger the strand-displacement reaction and sequentially activate the DNAzyme-assisted target recycling, leading to strong increase in corresponding fluorescence intensity for imaging. It enables to simultaneously assess multiplex cancer-related miRNAs abundance, even if at a very low expression level, in different cells through the different fluorescence intensities due to the dual signal amplification, and abundance change of miRNA induced by siRNA or mimic miRNAs in living cells can also be efficiently monitored. The versatile and responsive DNA hydrogel system holds great potential for miRNA biomedical application.

[*] X. Meng, K. Zhang, W. Dai, Y. Cao, F. Yang, Prof. Dr. H. Dong, Prof. Dr. X. Zhang

Beijing Advanced Innovation Center for Materials Genome Engineering

University of Science and Technology Beijing

30 Xueyuan Road, Beijing 100083 (P. R. China)

E-mail: zhangxueji@ustb.edu.cn or hfdong@ustb.edu.cn

X. Meng, K. Zhang, W. Dai, Y. Cao, F. Yang, Prof. Dr. H. Dong, Prof. Dr. X. Zhang

Beijing Key Laboratory for Bioengineering and Sensing Technology, Research Center for Bioengineering and Sensing Technology

School of Chemistry and Biological Engineering, University of Science & Technology Beijing

30 Xueyuan Road, Beijing 100083 (P. R. China)

E-mail: *hfdong@ustu.edu.cn* and *zhangxueji@ustb.edu.cn*

Materials and reagents:

Copper (II) chloride dihydrate ($CuCl_2 \cdot 2H_2O$), magnesium chloride hexahydrate ($MgCl_2 \cdot 2H_2O$), zinc chloride ($ZnCl_2$) and trisodium citrate dihydrate were purchased from Sinopharm Chemical Reagent Co., Ltd (Shanghai, China). Tetrachloroauric acid ($HAuCl_4$) was provided by Toronto Research Chemicals Inc. (Toronto, Canada). All the reagents were of analytical reagent grade. Ultrapure water generated from the Millipore Milli-Q water purification system (Billerica, MA, USA) was used in all experiments. Phosphate-buffered saline (PBS, pH 7.4, 10 mM, 137 mM NaCl), Dulbecco's modified Eagle's medium (DMEM) and fetal bovine serum (FBS) were provided by Life Technologies Corporation (Los Angeles, CA, USA). The oligonucleotides strands in our experiments were obtained by Sangon Biological Engineering Technology & Services Co., Ltd. (Shanghai, China). All of the nucleotides strands were purchased from GenePharma (Shanghai, China) and diluted in diethy pyrocarbonate (DEPC) water for further use. The sequences were presented as follows:

Sequences of DNA strands (5'- to 3'-):
P1 (for miR-21):
TACTCTCGG**rA**TCAACATCAGTCTGATAAGCTA
H1 (Cu^{2+}, for miR-21):
CTTATCAGACTGATGTTGATGGGCCTCTTTCTTTTTAAGCGAGAGTATCTTT
TTCAGTCTGATAAG
P2 (for miR-373):
ACTACTAGG**rA**TACACCCCAAAATCGAAGCACTTC
H2 (Mg^{2+}, for miR-373):
GCTTCGATTTTGGGGTGTACAGCGATTCCGGAACGGACACCCATGTCTAG
TAGTTACTTTTCAAAATCGAAGC
P3 (for miR-155):
ATCACTGGG**rA**TCCCCTATCACGATTAGCATTAA
H3 (Zn^{2+}, for miR-155):
ATGCTAATCGTGATAGGGGACTCCGAGCCGGTCGAAACAGTGATTCCTTT
TTCACGATTAGCAT
T1:
GGTGTACTAGTAGTAATTGACGAGAGTAAAA**G*G*G*G*G*T*G*G*G*G*G***AAATAGCTTATCAGA CAAGAAGTGCTTCGA T
T2:
TTAATGCTAATCGAAGGTGTACTAGTAGTAAA**G*G*G*G*G*T*G*G*G*G*G***AAAGAAGTGCTTCGATAAGGGG ACCAGTGAT
T3:

TTGACGAGAGTAAAGGGGACCAGTGATAAA**G*G*G*G*G*T*G*G*G*G*G**
*AAATAGCTTATCAGACAATTAATGCTAATCG
P1 for agarose gel electrophoresis:
TACTCTC GGAT CAA CAT CA G TCT GAT AAG CTA
P2 for agarose gel electrophoresis:
ACTACTA GGAT AC ACC CCA AA A TCG AAG CAC TTC
P3 for agarose gel electrophoresis:
ATCACTG GGAT C CCC TAT CA C GAT TAG CAT TAA
T1 for agarose gel electrophoresis:
GGT GT AC TAGTAGTAA TTG A C GAGAGTA
T2 for agarose gel electrophoresis:
TTA ATG CTA ATC G AA GGT GT A C TAGTAGT
T3 for agarose gel electrophoresis:
TTG AC GAGAGTA AA GGG G A C CAGTGAT
Note: The red portion refers to ribonuclease-modified site. The basic groups with * indicate phosphorothioate linkage.

Sequences of RNA strands (5'- to 3'-):
miR-21: UAG CUU AUC AGA CUG AUG UUG A
miR-21 mimics (double strands):
UAGCUUAUCAGACUG AUGUUGA/AACAUCAGUCUGAUAAGCUUC
miR-21 inhibitor (signal strand): UCAACAUCAGUCUGAUAAGCUA
miR-373: GAA GUG CUU CGA UUU UGG GGU GU
miR-373 mimics (double strands):
GAAGUGCUUCGAUUUUGGGGUGU/ACCCCAAAAUCGAAGCACUUCCU
miR-373 inhibitor (signal strand): ACACCCCAAAAUCGAAGCACUUC
miR-155: UUA AUG CUA AUC GUG AUA GGG G
miR-155 mimics (double strands):
UUAAUGCUAAUCGUGAUAGGGG/CCUAUCCACGAUUAGCAUUAAUU
miR-155 inhibitor (signal strand): CCCCUAUCACGAUUAGCAUUAA

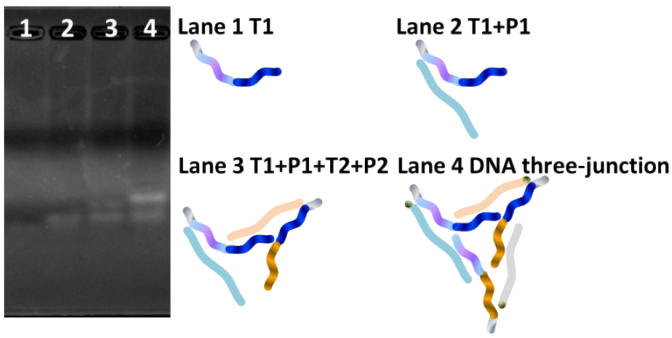

Fig. S1. The assemble process of DNA three-junction for constructing the AuDH.

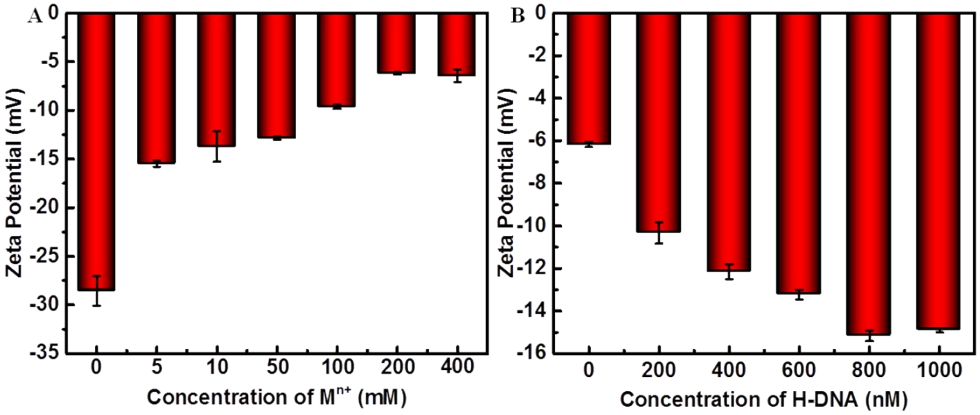

Fig. S2. The loading capacities of AuDH for metal ions (A) and hairpin-locked DNAzyme strands (B).

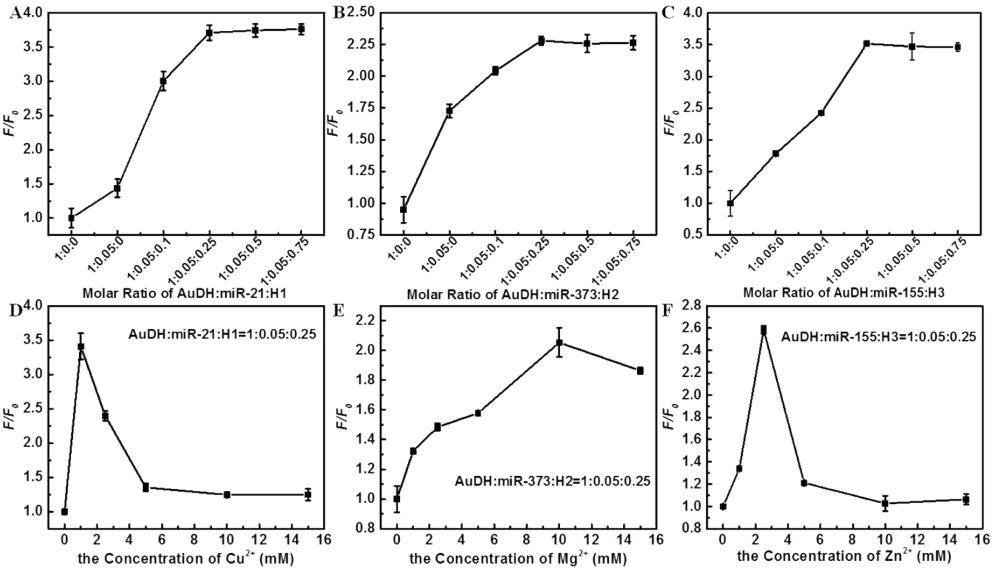

Figure S3. (A-C) The influence of H to miRNAs detection in the conditions that the concentrations of the AuDH, miRNA and metal irons were 0.5 mM, 0.025 mM and 5 mM, respectively. (D-F) The influence of metal irons (Cu^{2+}, Mg^{2+} and Zn^{2+}) to miRNAs detection in the conditions that the concentrations of the AuDH, miRNA and H were 0.5 mM, 0.025 mM and 0.125 mM, respectively.

As shown in **Figure S3A-C**, the molar ratio of AuDH and target miRNA was fixed at 1:0.05 and the concentrations of metal irons were all chosen as 5 mM. The ratio of F and F_0 (F_0, the fluorescence intensity of AuDH/M^{n+}) increased long with the increase of hairpin-locked DNAzyme strands concentration and reached to a plateau when the molar ratio of AuDH:miRNA:H was 1:0.05:0.25. The concentrations of Cu^{2+}, Mg^{2+} and Zn^{2+} were also optimized under the conditions that the molar ratio of AuDH, target miRNA and hairpin-locked DNAzyme strands was 1:0.05:0.25. The optimal concentration of Cu^{2+}, Mg^{2+} and Zn^{2+} was 1 mM, 10 mM and 2.5 mM (**Figure S3D-F**).

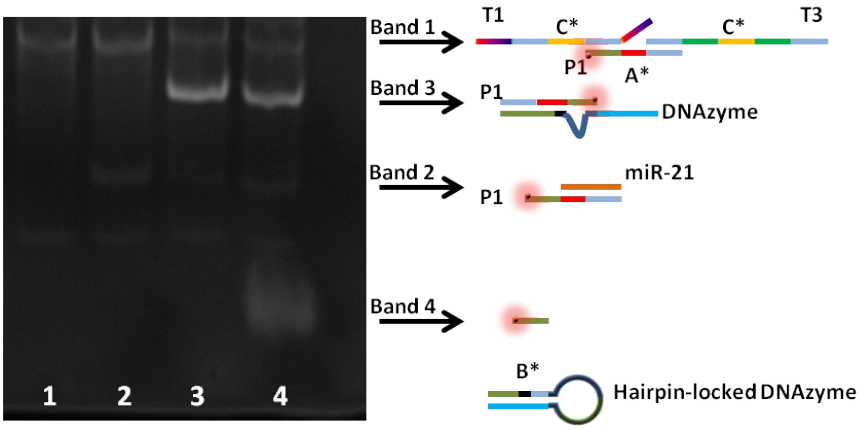

Fig. S4 The polyacrylamide gel electrophoresis presenting the feasibility of the strand-displacement reaction and hairpin-locked DNAzyme-assisted dual-signal amplification. Lane 1: T1-P1-P3; Lane 2: T1-P1-P3 and miR-21; Lane 3: T1-P1-P3, miR-21 and H1; Lane 4: T1-P1-P3, miR-21, H1 and Cu^{2+}.

miRNA-21: UAG CUU AUC AGA C UG AUG UUG A

P1: FAM-TACTCTC GGrAT CAA CAT CA G TCT GAT AAG CTA

H1 (Hairpin-locked DNAzyme):

*CTTATCAGACTGA*TGTTGATGGGCCTCTTTCTTTTTAAGCGAGAGTATCTTTT

TCAGTCTGATAAG

In the absence target, the P1 strand in the T1-P1-T3 structure just has two bases (the red letters with underline) available for H1 recognition, which could not effectively induce the hybridization and displacement reaction to form the DNAzyme for Cu^{2+} recognition. In presence of target miR-21, P1 hybridized with miR-21 through the site of miR-21 recognition (the red letters, 5 bases) to form P1/miRNA-21 duplex structure and expose the site (the green letters, 8 bases) for effective H1 recognition on the P1 strand.

As shown in **Fig. S4**, polyacrylamide gel electrophoresis analysis was performed to verify the dual signal amplification. The T1-P1-T3 structure was formed by the annealing of T1, P1 and T3 strands, resulting in a band (top in Lane 1) with a high molecular weight (MW). In the presence of target miR-21, the P1 hybridized with miR-21 (band 2, Lane 2). When the H1 was added into the mixture of miR-21 and T1-P1-T3 (Lane 3), an obvious new band was obtained (band 3). The adding of miR-21,

H1 and Cu^{2+} (Lane 3) into T1-P1-T3, the lowest band (band 4) was clearly observed in Lane 4, which was assigned to DNA fragment from hairpin-locked DNAzyme nicking.

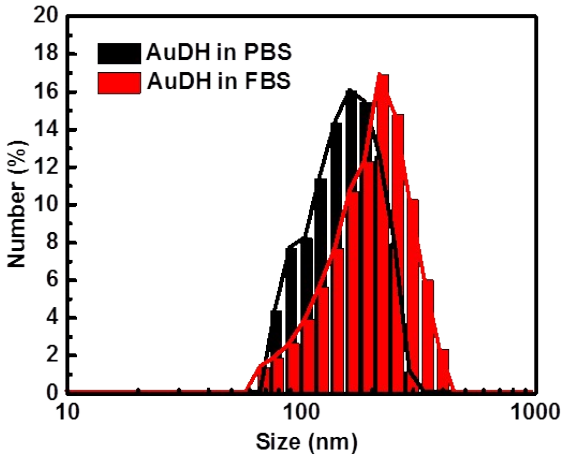

Fig. S5 DLS of AuDH in PBS (pH 7.4, 10 mM) and in FBS, respectively

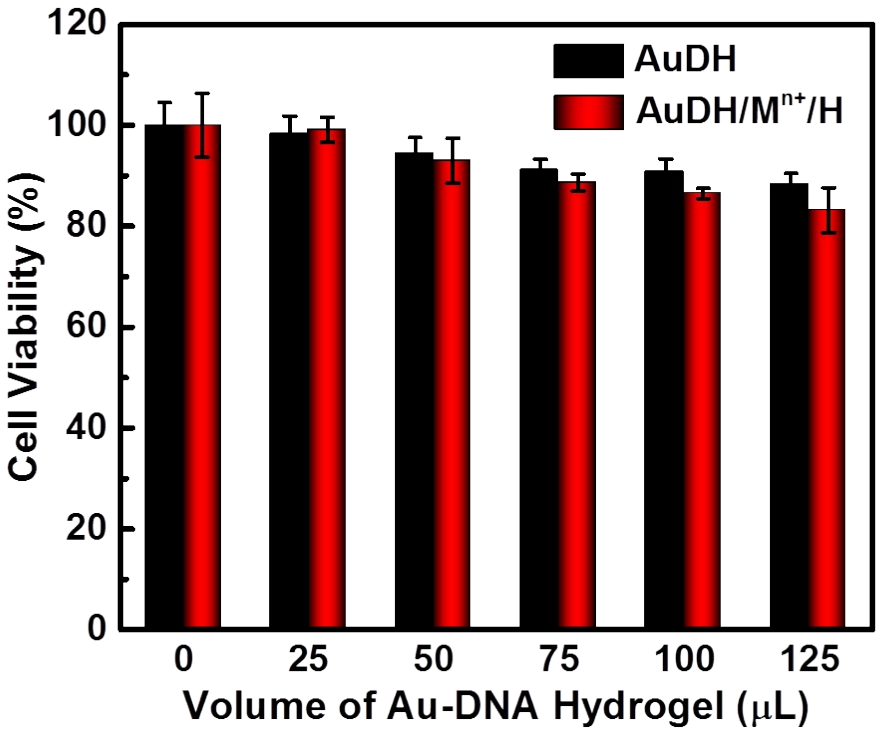

Fig. S6 The cytotoxicity of MCF-7 cells incubated with different volume of hydrogels (0-125 μL) in DMEM.

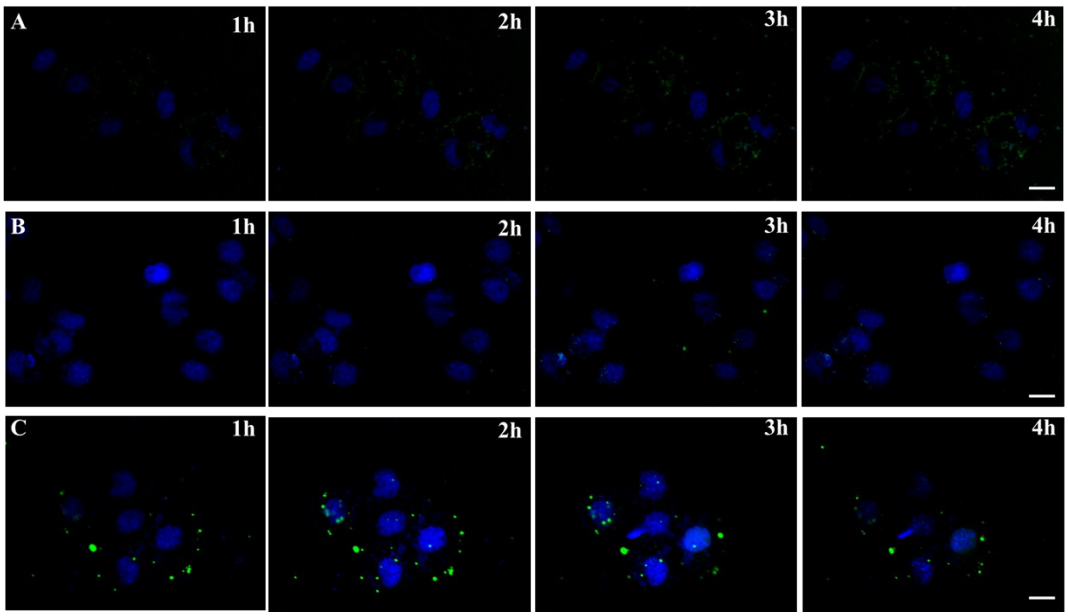

Fig. S7 The cellular uptake of the prepared AuDH (A), DNA-hydrogels (B) and commercial Lipofectamine®2000 (C) in MCF-7 cells.

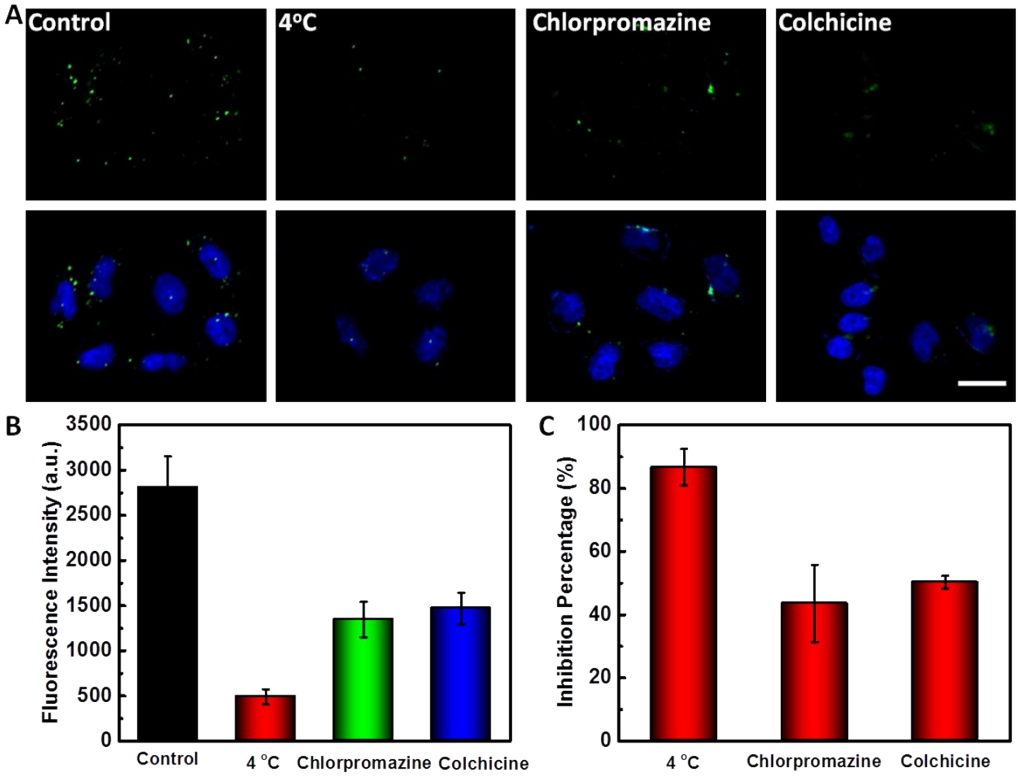

Fig. S8 (A) The CLSM images of MCF-7 cells incubated with FAM-labeled AuDH. MCF-7 without any treatment was regarded as control. (B) The corresponding fluorescence intensities of MCF-7 cells incubated with FAM-labeled AuDH. (C) The inhibition effect of low temperature (4°C), chlorpromazine and colchicine on the cellar uptake of FAM-labeled AuDH.

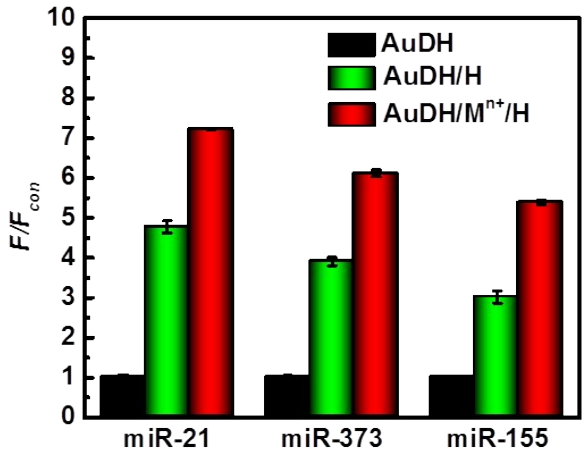

Fig. S9 The corresponding fluorescence intensities of the AuDH, AuDH/H and AuDH/M^{n+}/H in MCF-7 cells.